TISSUE ENGINEERING: Part A
Volume 15, Number 00, 2009

DOI: 10.1089/ten.tea.2008.0461

The Effect of Perfluorocarbon-Based Artificial Oxygen Carriers on Tissue-Engineered Trachea

Qiang Tan, M.D.,[1,2] Ashraf Mohammad El-Badry, M.D.,[3,4] Claudio Contaldo, M.D.,[5] Rudolf Steiner, M.D.,[6] Sven Hillinger, M.D.,[7] Manfred Welti, B.Sc.,[1] Monika Hilbe, V.M.D.,[8] Donat R. Spahn, M.D.,[9] Rolf Jaussi, Ph.D.,[10] Gustavo Higuera, M.Sc., B.Sc.,[11] Clemens A. van Blitterswijk, Ph.D.,[11] Qingquan Luo, M.D.,[2] and Walter Weder, M.D.[7]

The biological effect of the perfluorocarbon-based artificial oxygen carrier (Oxygent™) was investigated in tissue-engineered trachea (TET) construction. Media supplemented with and without 10% Oxygent were compared in all assessments. Partial tissue oxygen tension (PtO_2) was measured with polarographic microprobes; epithelial metabolism was monitored by microdialysis inside the TET epithelium perfused with the medium underneath. Chondrocyte–DegraPol® constructs were cultured for 1 month with the medium before glycosaminoglycan assessment and histology. Tissue reaction of TET epithelial scaffolds immersed with the medium was evaluated on the chick embryo chorioallantoic membrane. Oxygent perfusion medium increased the TET epithelial PtO_2 (51.2 ± 0.3 mm Hg vs. 33.4 ± 0.3 mm Hg at 200 μm thickness; 12.5 ± 0.1 mm Hg vs. 3.1 ± 0.1 mm Hg at 400 μm thickness, $p < 0.01$) and decreased the lactate concentration (0.63 ± 0.08 vs. 0.80 ± 0.06 mmol/L, $p < 0.05$), lactate/pyruvate (1.87 ± 0.26 vs. 3.36 ± 10.13, $p < 0.05$), and lactate/glucose ratios (0.10 ± 0.00 vs. 0.29 ± 0.14, $p < 0.05$). Chondrocyte–DegraPol in Oxygent group presented lower glycosaminoglycan value (0.03 ± 0.00 vs. 0.13 ± 0.00, $p < 0.05$); histology slides showed poor acid mucopolysaccharides formation. Orthogonal polarization spectral imaging showed no difference in functional capillary density between the scaffolds cultured on chorioallantoic membranes. The foreign body reaction was similar in both groups. We conclude that Oxygent increases TET epithelial PtO_2, improves epithelial metabolism, does not impair angiogenesis, and tends to slow cartilage tissue formation.

Introduction

The history of trachea replacement dates back to the 19th century, yet till today no clinically convincing method has been established.[1] Tissue engineering has emerged as a promising approach, while hypoxia remains as one of the major obstacles for the success in construction of tissue-engineered trachea (TET).[2,3] During the generation of large-size cell–scaffold constructs, cells near the surface are able to receive sufficient oxygen and nutrients through diffusion from immersed medium (*in vitro*) or from surrounding tissue fluid (*in vivo*), whereas cells located in the center are often subjected to detrimental hypoxic conditions.[4–7] Previous studies showed that oxygen delivery by diffusion supports only less than 100-μm-thick tissues, and it is hypothesized that continuous medium perfusion may extend these limitations by combining diffusion and convection.[8] Such being the case, in our research of TET we propose an *in vivo* bioreactor concept defined as implanted tissue-engineered substitutes integrated with an intrascaffold medium flow created by an extracorporeal portable pump system for *in situ* organ regeneration.[8–10] Acting like a topical heart lung machine, the *in vivo* bioreactor device aims to maintain the survival of preseeded chondrocytes and epithelia until nutritional vessels growing deeply into the TET from surrounding tissues. Through this special design, we aim

[1]Laboratory of Tissue Engineering, Department of Thoracic Surgery, University Hospital Zurich, Zurich, Switzerland.
[2]Shanghai Lung Tumor Clinical Medical Center, Shanghai Chest Hospital, Shanghai, China.
[3]Department of Visceral and Transplant Surgery, University Hospital Zurich, Zurich, Switzerland.
[4]Department of General Surgery, Sohag Faculty of Medicine, Sohag University Hospital, Sohag University, Sohag, Egypt.
[5]Department of Plastic, Reconstructive, and Hand Surgery; [6]Department of Oncology; [7]Department of Thoracic Surgery; University Hospital Zurich, Zurich, Switzerland.
[8]FVH (Pathology), ECVP Institute of Veterinary Pathology, Zurich, Switzerland.
[9]Institute of Anesthesiology, University Hospital Zurich, Zurich, Switzerland.
[10]Biomolecular Research, Paul Scherrer Institute, Villigen PSI/Switzerland.
[11]Department of Tissue Regeneration, University of Twente, Enschede, The Netherlands.

to combine traditionally separated *in vitro* reconstruction and *in vivo* regeneration steps in tissue engineering research and treat the patient as the bioreactor for her/his own tissue-engineered organ.

To further increase the oxygen delivery to the implanted TET, we searched for an artificial oxygen carrier that could supplement the perfusion medium of the *in vivo* bioreactor. According to the oxygen dissociation curve of normal blood, at 100 mm Hg partial pressure of oxygen, 98.5% oxygen (19.7 mL/100 mL) is carried by hemoglobin, whereas the oxygen dissolved in plasma, similar to that in medium, is only around 0.3 mL/100 mL. Oxygent™ (Alliance Pharmaceutical Corp., San Diego, CA), an improved second-generation perfluorocarbon (PFC), is an emulsion based on perflubron (perfluorooctylbromide; C8F17Br), and it is a highly stable molecule that can carry over 20 times more oxygen than plasma.[11] Numerous studies thus far carried out have investigated the capability of PFC as a gas-carrying pharmacological agent for cardiovascular and respiratory applications to increase the tissue oxygen tension.[12–14]

Mimicking normal tracheal structure, the TET prosthesis suitable for *in vivo* bioreactor design consisted of three layers: epithelial layer composed of tracheal epithelium and acellular dermal matrices (ADM); submucous layer founded by porous poly(ethylene oxide terephthalate)-poly(butylene terephthalate) (PEOT/PBT) scaffold with continuous medium perfusion; cartilage layer constituted from chondrocyte–DegraPol® constructs providing sufficient mechanism strength. In this study, the TET epithelial partial tissue oxygen tension (PtO_2) level was assessed by polarographic microprobes, and the epithelial metabolism was measured by continuous microdialysis of glucose and lactate concentration, as well as lactate/glucose (L/G) and lactate/pyruvate (L/P) ratios under medium perfusion with and without Oxygent. The effects of Oxygent emulsions on formation of cartilage tissue in chondrocyte–DegraPol constructs were investigated by glycosaminoglycan (GAG) assessment and histology.[15,16] The effect of Oxygent on TET epithelial scaffold neovascularization was investigated *in vivo* on the chorioallantoic membrane (CAM) of the chick embryo with orthogonal polarization spectral (OPS) imaging.[17–19] The *in vivo* reactions of CAM tissue to the transplants were analyzed by histology for the presence of acute/chronic inflammation, foreign body reaction, and fibrosis.

Materials and Methods

Agents

Oxygent emulsion (50 mL), supplied by Alliance Pharmaceutical (San Diego, CA) was mixed with culture medium (DMEM—Dulbecco's Modified Eagle's Medium—or F12) 450 cc to obtain 10% w/v of Oxygent medium, and thereafter, it was referred to as Oxygent–DMEM or Oxygent–F12, respectively. Rectangular (20×10×2 mm) PEOT/PBT scaffolds were obtained from IsoTis S.A. (Bilthoven, The Netherlands) in a composition denoted as 300/55/45 (300 = PEG MW (g/mol), 55/45 = wt% of PEOT/PBT-blocks).[20] Tubular DegraPol scaffolds (Bioengineering Laboratories, Cantu, Italy), 1 cm in length with 2 mm inner diameter and 6 mm outer diameter, were biodegradable polyesterurethane foam processed into an open porous structure by a freeze-precipitation technique with pore sizes in the range of 150–200 μm.[21] The IPC high-precision multichannel peristaltic pumps and Tygon Long Flex Life (LFL) tubing (1.6 mm inner diameter) were purchased from Ismatec (Zurich, Switzerland). Xenogenic (porcine) ADM, 20×20×0.2 mm, were provided by Jiangshu Qidong Institute of Medical Supplies (Jiangshu, China).[22] Transwell permeable supports (six-well plate, 8 μm pore size polycarbonate membrane) were purchased from Corning (New York, NY).

Oxygent effect on TET epithelium

PtO_2 measurements in TET epithelium. The TET epithelium was assembled as previously published by our group.[9] Briefly, human tracheal epithelial cell line 16HBE14o cultured in DMEM was harvested and seeded onto ADM in a concentration of 1×10^7/mL. The cell–scaffold constructs were then cultured with an air–liquid interface in six-well Transwell permeable supports for 1 week with medium changes every other day. The constructs were then folded (to pinch one microprobe) and placed on the surface of a rectangular porous PEOT/PBT scaffolds to form a simple test model of a reepithelialized TET patch. A continuous medium flow was formed inside the PEOT/PBT scaffold with two inserted needles, which were connected to two peristaltic pumps through LFL tubes. One inlet pump continuously delivered the medium into the scaffold, whereas the other outlet pump discarded the waste.

Epithelial PtO_2 was assessed with Clark-type microprobes consisting of polarographic electrodes and an oxygen-sensitive microcell (Revoxode CC1; Integra, Kiel, England).[23] During the PtO_2 measurement, to prevent the oxygen exchange between the intrascaffold medium and air, the TET patch under perfusion was wrapped in rat skin tissue. The TET epithelium was folded around one polarographic microprobe to obtain PtO_2 values reflecting the 200-μm-thick TET epithelium (amounting to the thickness of one layer of ADM). A second polarographic microprobe was placed between the TET epithelium and the rat skin tissue for analysis of PtO_2 in 400-μm-thick TET epithelium (amounting to the thickness of two layers ADM) (Fig. 1).

During the measurements, six TET patch samples were randomly assigned into two groups perfused with DMEM or Oxygent–DMEM described under (i) continuous perfusion for 30 min, (ii) interrupted perfusion for 30 min, and (iii) restarted perfusion for 30 min. The perfusates were then reoxygenated with pure oxygen for 10 min, and the procedure was repeated. All the measurements were performed in an incubator at 37°C with 5% CO_2.

Metabolite monitoring by microdialysis in TET epithelium. Epithelial metabolism was measured by microdialysis probes (CMA/20, CMA Microdialysis AB) with a molecular weight cut-off of 20,000 Da and a membrane length of 5 mm.[23] Six pieces of TET epithelium were randomly assigned to the DMEM and Oxygent–DMEM perfusion groups. The TET epithelium was wrapped around the microdialysis probe before being placed on top of a PEOT/PBT scaffold perfused with DMEM or Oxygent–DMEM as described above. The TET patch was left unwrapped to mimic the physiological air exposure situation of tracheal epithelium. The probes were equilibrated for 1 h, followed with continuous measurements of glucose, lactate, and pyruvate concentrations for 8 h.

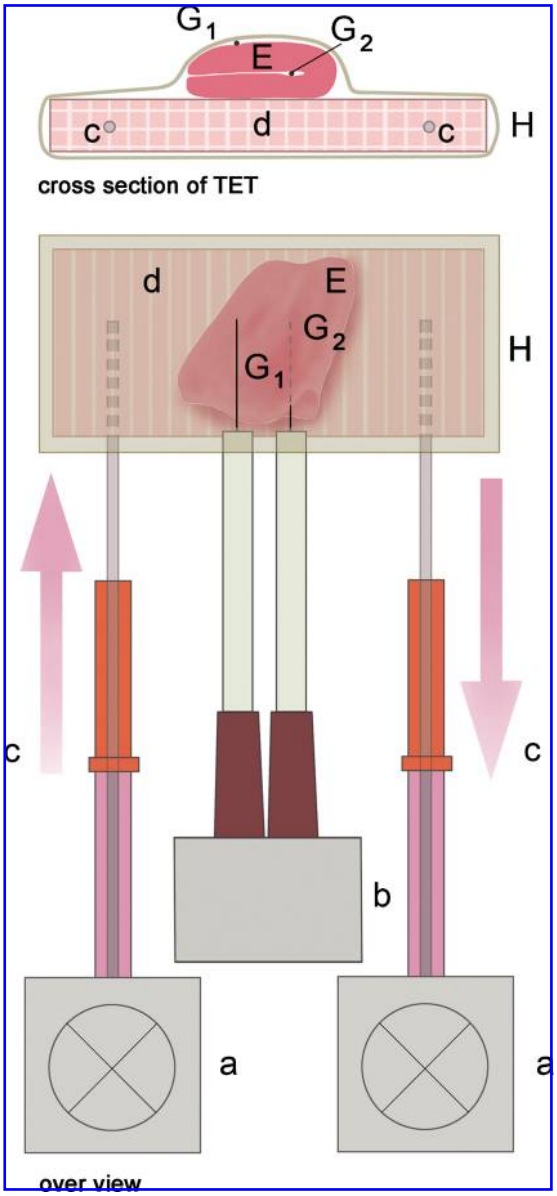

FIG. 1. Schematic diagram shows experimental setting for TET epithelial PtO_2 measurements. (**a**) peristaltic pump; (**b**) Clark-type microprobes; (**c**) direction of perfusion flow to and from the TET; (**d**) rectangular porous PEOT/PBT scaffold; (**E**) TETE; (**G1, G2**) probes for PtO_2 measurement: G1 placed on the surface of the TET epithelium and G2 inserted into the TET epithelium; (**H**) rat skin encircled the TET circumferentially preventing oxygen exchange with air. TET, tissue-engineered trachea; PtO_2, partial tissue oxygen tension; PEOT/PB, poly (ethylene oxide terephthalate)-poly (butylene terephthalate).

Oxygent effect on TET chondrocyte–DegraPol constructs

GAG assessments. Chondrocyte–DegraPol constructs were constructed as previously described by our group.[21] A total of 10 tubular DegraPol scaffolds were seeded with 1×10^7/scaffold rat chondrocytes and stored in an incubator for 2 h to facilitate cell attachment. The cell–scaffold constructs were then assigned randomly into two groups, cultured in F12 and Oxygent–F12, respectively, for 1 month during which the medium was changed twice per week. The GAG measurements followed the standard protocol described in the literature.[24]

Histological analysis. Chondrocyte–DegraPol samples were fixed with 4% phosphate-buffered formalin, embedded in paraffin, and sectioned using standard histological techniques. Sections were stained with hematoxylin and eosin (H&E), as well as with Alcian blue and Toluidine Blue/Fast Green, to detect acid mucopolysaccharides.

Oxygent effect on ADM scaffold tissue reactions in the CAM model

Microvascular response (OPS imaging). The *ex ovo* chick embryos CAM model was chosen to assess the effect of Oxygent emulsion deposits on tissue reactions of ADM scaffolds.[25] For this purpose, five fertilized chicken eggs were opened at incubation day (ID) 3, and the contents were gently poured into 25×100 mm plastic cups without damaging the yolk sac and embryo. Each *ex ovo* chick embryo was transferred to a 38°C incubator with 90% humidity for subsequent 6 days until the CAM was sufficiently developed. On ID 9, two ADM scaffolds preimmersed for 12 h in DMEM and Oxygent–DMEM, respectively, were placed onto the surface of the CAMs. Before being harvested, the ADM transplants (ADM and ADM-Oxygent scaffolds) on the CAMs were incubated for another 10 days and kept moist twice per day with the corresponding medium.

At ID 19, the angiogenic response around the ADM transplants was assessed by OPS imaging, using the Cytoscan device (Cytometrics, Philadelphia, PA). The probes were placed directly onto the CAM in the vicinity of the ADM transplants. The images were displayed on the Cytoscan screen and recorded on videotape for off-line analysis. Functional capillary density assessments were performed off-line by means of frame-to-frame analysis of the videotaped images using a computer-assisted image analysis system (CapImage; Zeintl, Heidelberg, Germany) as previously described.[26]

Histological evaluation. After OPS imaging, the ADM transplants placed on the top of the CAMs were fixed *in situ* with 4% phosphate-buffered formalin, embedded in paraffin blocks, and sectioned using standard histological techniques. Slides were stained with H&E. The histological evaluation included the presence or absence of inflammatory signs (acute to chronic), foreign body reaction, and fibrosis.[18]

Statistical analysis

All the data from the two groups were expressed as mean ± standard deviation, and statistical analysis performed by unpaired *t*-test at a given *p*-value of less than 0.05 was considered statistically significant. The semi-quantitative data regarding the foreign body reactions were assessed using the Chi-square test; $p < 0.05$ was considered significant.

Results

Oxygent effect on TET epithelium

PtO_2 measurements in TET epithelium. The TET epithelial PtO_2 measurement results are summarized in Figure 2.

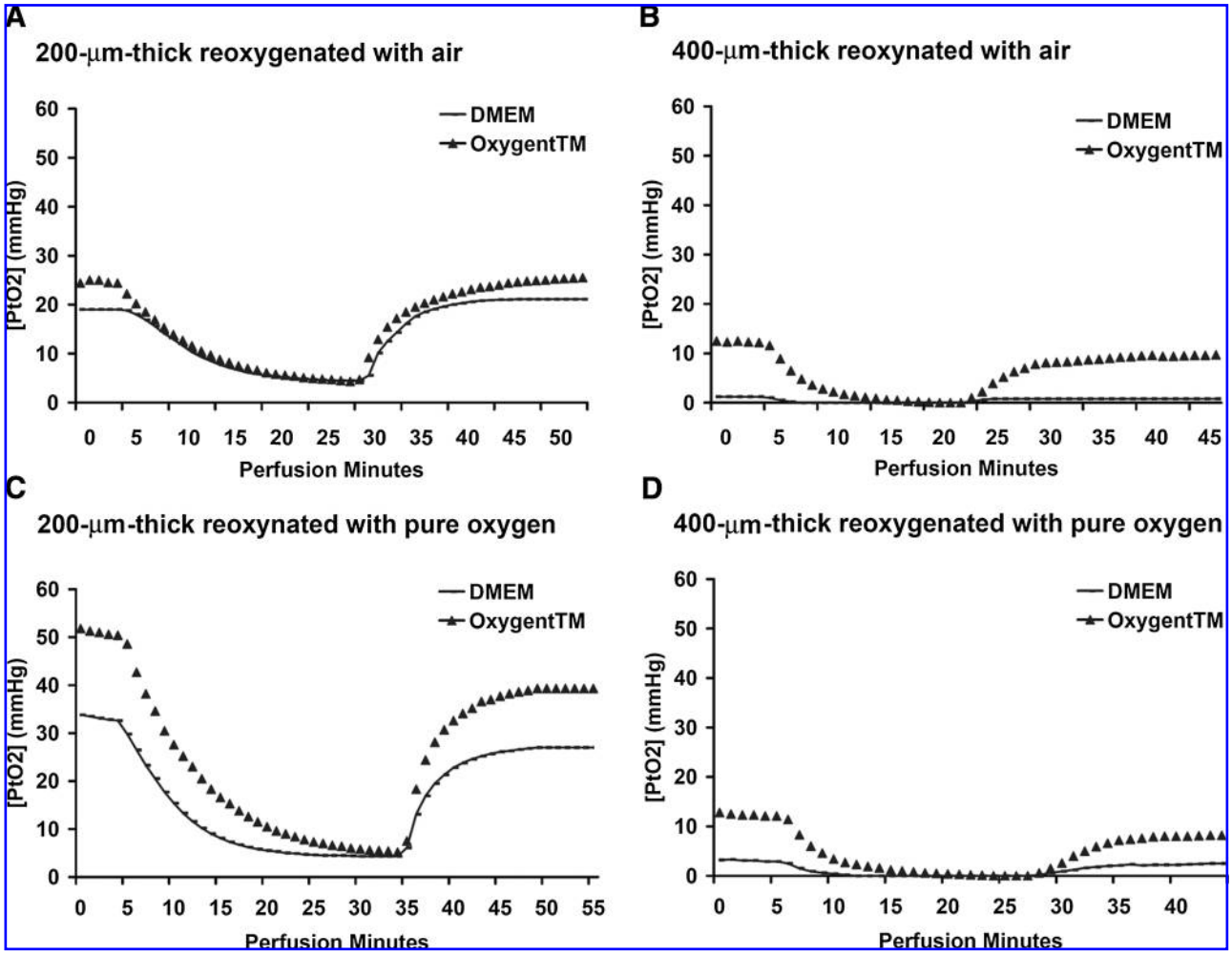

FIG. 2. PtO_2 measured in 200-μm-thick (**A, C**) and 400-μm-thick (**B, D**) TET epithelium with (▲) and without (-) Oxygent™ reoxygenated with air (**A, B**) and pure oxygen (**C, D**). (**A**) Reoxygenated with air Oxygent–DMEM perfusion provided 10% more oxygen and increased the PtO_2 level 5 mm Hg above the DMEM perfusion PtO_2 in 200-μm-thick TET epithelium. (**B**) Reoxygenated with air Oxygent–DMEM perfusion provided nearly 34 times more oxygen and increased the PtO_2 level 10 mm Hg above the DMEM perfusion PtO_2 in 400-μm-thick TET epithelium. (**C**) Reoxygenated with pure oxygen, Oxygent–DMEM perfusion provided nearly 74% more oxygen and increased the PtO_2 level 18 mm Hg above the DMEM perfusion PtO_2 in 200-μm-thick TET epithelium (reached physiological PtO_2 level). (**D**) Reoxygenated with pure oxygen, Oxygent–DMEM perfusion provided nearly six times more oxygen and increased the PtO_2 levels 9 mm Hg above the DMEM perfusion PtO_2 in 400-μm-thick TET epithelium. The Oxygent significantly increased the PtO_2 of TET epithelium and augmented the depth of tissue oxygen penetration. PtO_2, partial tissue oxygen tension; TET, tissue-engineered trachea; DMEM, Dulbecco's Modified Eagle's Medium.

Each figure contains two curves representing the changes of PtO_2 under perfusion of DMEM and Oxygent–DMEM, respectively. Each curve can be separated into three phases: phase I reflects the PtO_2 level under continuous medium perfusion; phase II represents the PtO_2 decrease pattern after the interruption of the perfusion; and phase III depicts the PtO_2 increase pattern after the medium perfusion was restarted. The data at every time point represent an average value calculated from three experiments.

Under continuous perfusion with DMEM reoxygenated by air, the PtO_2 level stabilized around 18.8 ± 0.1 mm Hg in 200-μm-thick TET epithelium and 1.1 ± 0.1 mm Hg in 400-μm-thick TET epithelium. The corresponding data under Oxygent–DMEM perfusion were 23.7 ± 0.7 mm Hg and 11.8 ± 0.5 mm Hg, respectively, and both showed a significant difference in comparison with the DMEM perfusion corresponding data ($p < 0.01$). After the interruption of the perfusion pump, the PtO_2 level declined at similar rate in both groups to 4.67 ± 0.07 mm Hg at 200-μm-thick TET epithelium, whereas in the 400-μm-thick TET epithelium, the PtO_2 level dropped precipitously within 3 min to 0 mm Hg in the DMEM perfusion group and lasting for nearly 20 min in the Oxygent perfusion group. When perfusion pump was restarted, the PtO_2 level increased at a rate of 15.50 mm Hg/min in the 200-μm-thick TET epithelium and at 0.08 mm Hg/min in the 400-μm-thick TET epithelium in the DMEM perfusion group. In the Oxygent–DMEM perfusion group, the upward rate was similar in the 200-μm-thick TET epithelium (17.50 mm Hg/min) and almost 10 times faster in the 400-μm-thick TET epithelium (0.81 mm Hg/min) than the upward rate in the

DMEM perfusion group. By measuring the area under phase II, we concluded increased oxygen content in the TET epithelium under the Oxygent–DMEM perfusion, gaining 10.34% extra at 200-μm-thick TET epithelium and 3427.44% at 400-μm-thick TET epithelium, respectively.

In case of continuous perfusion with DMEM reoxygenated with pure oxygen, the TET epithelial PtO_2 level reached 33.2 ± 0.2 mm Hg in the 200-μm-thick scaffold and 3.1 ± 0.01 mm Hg in the 400-μm-thick scaffold; after the interruption of the perfusion pump, the level dropped to 5.5 ± 0.1 mm Hg within 15 min and 0 mm Hg within 5 min for the 200-μm-thick and 400-μm-thick scaffolds, respectively. On restarting the perfusion cycle, the PtO_2 levels resumed at a rate of 21.40 mm Hg/min in the 200-μm-thick TET epithelium and 0.21 mm Hg/min in the 400-μm-thick TET epithelium. In the Oxygent–DMEM perfusion group, the PtO_2 level was 51.0 ± 0.3 mm Hg in the 200-μm-thick TET epithelium and 12.4 ± 0.1 mm Hg in the 400-μm-thick TET epithelium under continuous perfusion; it dropped to 5.5 ± 0.1 mm Hg within 25 min and to 0 mm Hg in 20 min, respectively; on restarting the perfusion pump, it resumed at a speed of approximately 29.5 mm Hg/min (200 μm thickness) and 0.76 mm Hg/min (400 μm thickness) within 15 min. There were significant differences regarding the PtO_2 levels and PtO_2 variations in all the three phases between the DMEM and the Oxygent–DMEM perfusion groups inside both the 200-μm-thick TET epithelium and the 400-μm-thick TET epithelium. By measuring the area under phase II, the oxygen content of the epithelium under Oxygent–DMEM perfusion was found to be 73.79% increased in the 200-μm-thick TET epithelium versus 607.22% in the 400-μm-thick TET epithelium compared with the DMEM perfusion only.

Monitoring of metabolites by microdialysis in TET epithelium. The TET epithelial metabolite concentrations under different medium perfusions for 8 h are summarized in Figure 3. The data at every time point represent an average value calculated from three experiments. The even curve indicated a homeostasis niche of TET epithelium under Oxygent–DMEM perfusion. Accordingly, the statistical analysis showed a significant increase in the DMEM perfusion group regarding the lactate concentration (0.63 ± 0.08 vs. 0.80 ± 0.06 mmol/L, $p < 0.05$), L/P ratio (1.87 ± 0.26 vs. 3.36 ± 10.13, $p < 0.05$), and L/G ratio (0.10 ± 0.00 vs. 0.29 ± 0.14, $p < 0.05$). The glucose concentration remained similar (6.25 ± 1.26 vs. 5.15 ± 6.71, $p > 0.05$) for both groups although the variability of the results in the Oxygent–DMEM perfusion group was borderline.

Oxygent effect on TET chondrocyte–DegraPol constructs

GAG assessment. All samples were harvested without contamination. The GAG data represent an average value calculated from five samples. The GAG results showed less extracellular matrix formation in the Oxygent–F12 culture group than that in the F12 culture group (0.03 ± 0.00 vs. 0.13 ± 0.00, $p < 0.05$) (Fig. 4).

Histological analysis. On histology, some of the samples from the F12 culture group of the chondrocyte–DegraPol construct showed multilayered cell aggregates consisting of spindle- or polygonal-shaped cells covering the surface of the DegraPol scaffolds (Fig. 5A). Most of the polygonal cells had a moderate amount of eosinophil, with slightly granular cytoplasm, or were surrounded by a moderate amount of pale blue ground substance and showed a large round nucleus (i.e., chondrocyte-like morphology). Toluidine/Fast Green and Alcian blue staining was positive in cells with chondrocyte morphology, indicating cartilage tissue formation function (Fig. 5B). Inside the scaffold some spindle cells were visible. Regarding the Oxygent–F12 group, spindle cells both in the lumen and on the edge of the lumen were visible. At the edge of the lumen, the cells formed a small band-like structure. All the cells were Toluidine/Fast Green and Alcian blue negative (Fig. 5C, D). These histological results were consistent with better chondrocyte growth and some cartilage tissue formation in the F12 culture group than in the Oxygent–F12 culture group.

Oxygent effect on ADM scaffold tissue reactions in the CAM model

Microvascular response (OPS imaging). All chicken embryos survived until ID 19, and OPS imaging detected no significant difference regarding the functional capillary density in CAMs between the ADM and the Oxygent–ADM groups. Representative OPS imaging pictures close to the respective ADM scaffolds are shown in Figure 6.

Histological evaluation. Histological evaluation showed various degrees of a chronic-active inflammatory process in both groups in the region where the scaffolds were in direct contact with the CAM (ulcerative lesions in the allantoic epithelium, ballooning degeneration of the allantoic epithelium, and infiltration with heterophils) (Fig. 7A). In some slides, the scaffolds were engulfed into the mesoderm where heterophilic leukocytes and macrophages aggregate, and some fibrosis, as well as few lymphocytes, and plasma cells were seen (Fig. 7B). The macrophages engulfing the scaffold indicate a foreign body reaction. The histological changes were summarized semiquantitatively in Table 1. The tissue reaction to ADM and ADM–Oxygent scaffolds showed no significant difference.

Discussion

In this study, a continuous intrascaffold perfusion by medium supplemented with PFC-based artificial oxygen

Table 1. Semiquantitative Summary of the CAM Tissue Reactions to ADM Versus ADM-Oxygent™ Scaffolds

Histology	*ADM–Oxygent*	*ADM*
Ballooning degeneration of the CAM epithelium	++ to +++	++
Ulcerative lesions of the allantoic epithelium	+	+
Heterophilic leukocytes	++	++
Macrophages (interpreted as foreign body reaction)	+ to ++	+
Fibrosis in the mesoderm	+	+
Lymphocytes, plasma cells	+	+
Bacteria	−	+

Score: +, mild; ++, moderate; +++, strong reaction.
CAM, chorioallantoic membrane; ADM, acellular dermal matrix.

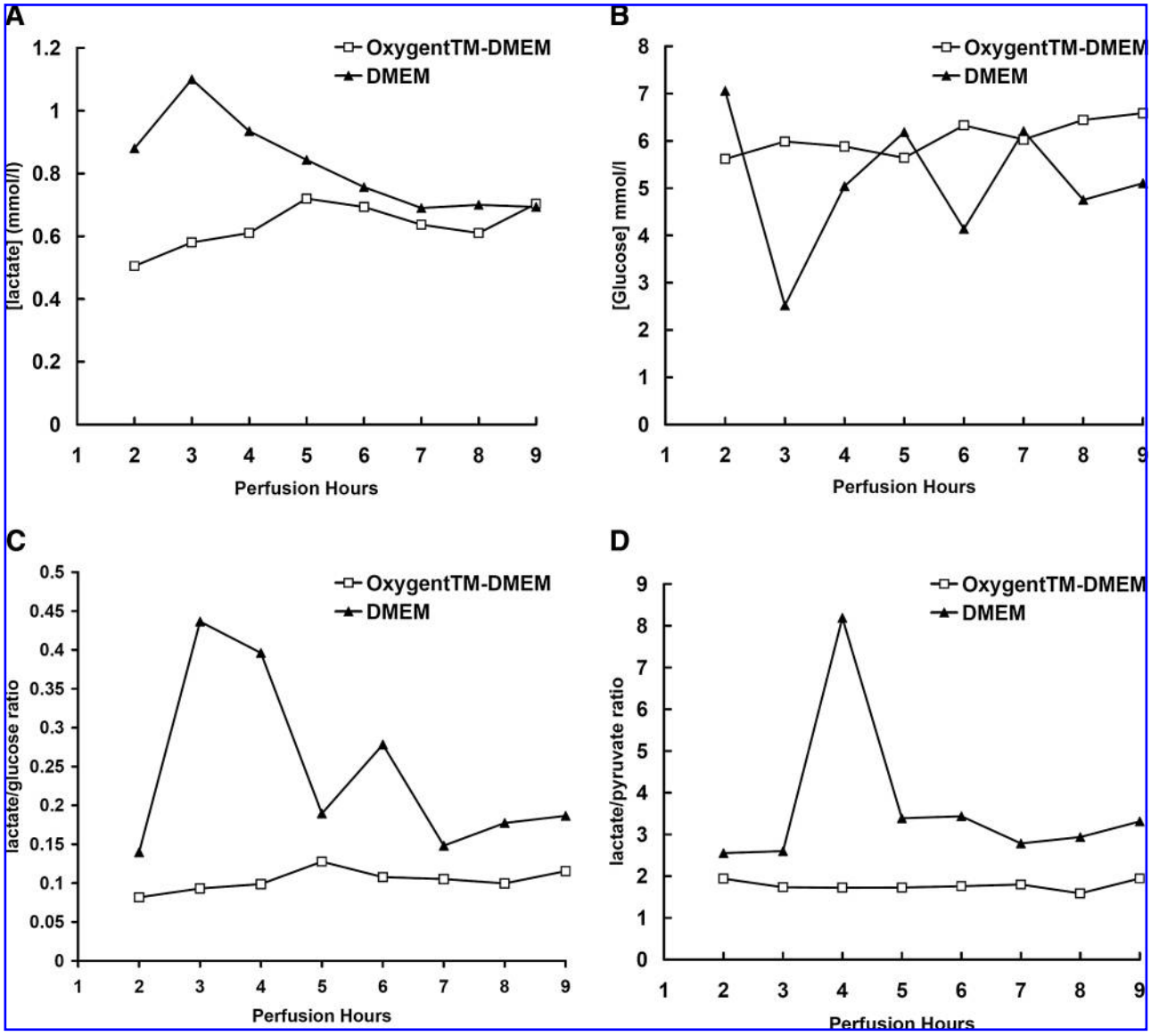

FIG. 3. Tissue metabolite concentrations measured by microdialysis in TET epithelium under medium perfusion with (□) and without (▲) Oxygent supplement. One hour after the start of perfusion, samples were collected continuously for 8 h. There were significant increases in the DMEM perfusion group for lactate concentrations (**A**) (0.63 ± 0.08 mmol/L vs. 0.80 ± 0.06 mmol/L, $p < 0.05$), L/P ratio (**D**) (1.87 ± 0.26 vs. 3.36 ± 10.13, $p < 0.05$), and L/G ratio (**C**) (0.10 ± 0.00 vs. 0.29 ± 0.14, $p < 0.05$). The glucose concentrations (**B**) remained similar (6.25 ± 1.26 vs. 5.15 ± 6.71, $p > 0.05$) for both groups although the data variance of the Oxygent–DMEM perfusion group was significantly small (0.13 vs. 1.99). These results were indicative for the optimized oxidative energy metabolism and cell niche homeostasis under Oxygent perfusion.

carrier (Oxygent) significantly increased the PtO_2 level of TET epithelium that, after implantation, is known to be sensitive to ischemia and bacterial invasion that induces an inflammation reaction leading to granulation tissue overgrowth followed by airway obstruction or bacteria colonization that could in turn cause lethal pneumonia.[1,10,27] According to the previously proposed mathematical model for oxygen distribution of Oxygent in cardiac tissue engineering by Radisic *et al.*, the gas solubility increased linearly with the gas partial pressure, and the PtO_2 level decreased proportionately with the thickness of the tissue supported by a single perfusion channel.[8,28] Therefore, TET epithelium thickness and the partial pressure of oxygen were chosen as two study parameters for monitoring the oxygen delivery efficacy both in the static cultures and under continuous perfusion. Our data showed that in the condition of conventional *in vitro* static cultures the PtO_2 levels in 200-μm-thick TET epithelium were much lower than the physiological PtO_2 levels (4.87 ± 0.11 mm Hg vs. 20–40 mm Hg) regardless of Oxygent addition.[23] However, under continuous perfusion, when oxygen is transported by both diffusion and convection, the PtO_2 levels increased by four- to five-fold to 18.83 ± 0.14 mm Hg (DMEM perfusion group) and 23.67 ± 0.68 mm Hg (10% w/v Oxygent–DMEM perfusion group). Although there was a significant difference between the two groups, the benefit of the Oxygent supplement proved to be limited when reoxygenated with air. Previous

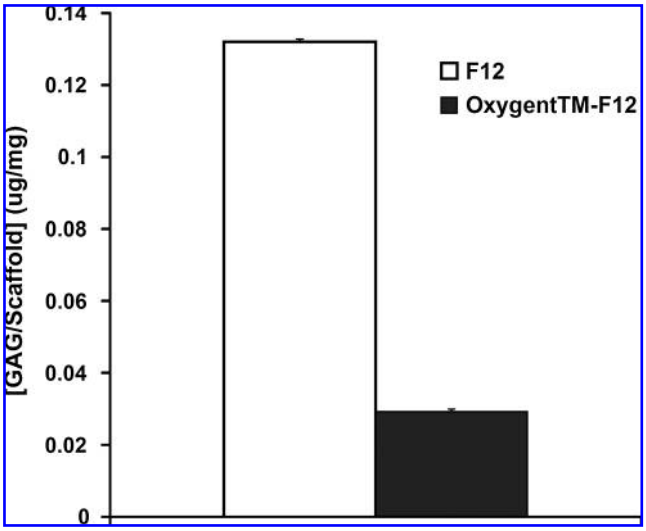

FIG. 4. GAG results of chondrocyte–DegraPol® constructs cultured in F12 medium with (■) and without (□) Oxygent. The F12 group showed much higher GAG values (0.03 ± 0.00 vs. 0.13 ± 0.00, $p < 0.05$). GAG, glycosaminoglycans.

Oxygent clinical studies have showed an optimal tissue oxygenation efficacy for patients breathing in an oxygen-enriched atmosphere. In subsequent experiments we oxygenated the perfusion medium with pure oxygen, and the results from the Oxygent–DMEM group showed raised PtO_2 values reaching physiological levels of 51.05 ± 0.25 mm Hg in the 200-μm-thick TET epithelium, whereas in the 400-μm-thick TET epithelium the PtO_2 level only increased to 10 mm Hg. Accordingly, the extra oxygen content in the Oxygent supplemented medium slowed the decrease of PtO_2 during the nonperfused interval followed with accelerated PtO_2 values upon reperfusion. On the basis of these data we conclude that a continuous intrascaffold perfusion with Oxygent could oxygenate 200- to 300-μm-thick TET epithelial tissues. This working distance should be enough to support the basal cell layer of split thickness skin graft in the future *in vivo* bioreactor application. Normal functional basal cells will prevent the overgrowth of granulation tissue and maintain the intact of basement membrane, which will prevent lethal airway obstruction and guide the recovery of ciliated tracheal epithelial. Our study also imply that if we want to make parallel channels in the tissue-engineered organ for artificial oxygen carrier perfusion, such as the model established by R. Langer, the distance between the channels should be less than 800 μm.[8]

The TET epithelial microdialysis results further underlined the advantage of Oxygent-containing medium. The improved oxidative energy metabolism under Oxygent perfusion correlated with a significant decrease of the lactate concentration, the L/P ratio, and the L/G ratio in the 200-μm-thick TET epithelium. Although there was a quantitative statistically significant difference, qualitatively the TET epithelium in both perfusion groups showed an aerobic cell metabolism. The difference might be obscured by the physiological air exposure of the TET epithelium during the measurements, which suggests that an advantage of artificial oxygen carrier applications might only fully emerge overtime. In this case, microdialysis was shown to be a reliable, readily applicable, and nondestructive method to monitor TET epithelial metabolism.

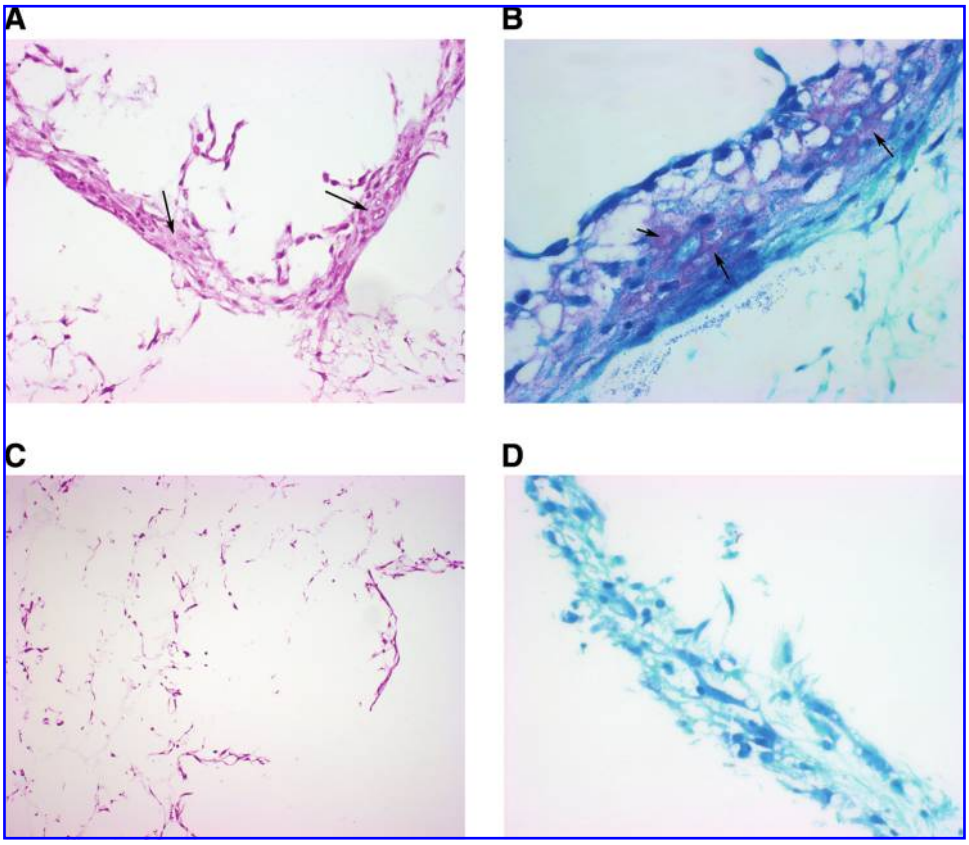

FIG. 5. Histology results of chondrocyte–DegraPol constructs cultured in F12 medium with (**C, D**) and without (**A, B**) Oxygent. (**A**) Spindle to polygonal-shaped cells (marked with arrows) resembling chondrocytes formed a multilayered cell aggregate on the surface of the DegraPol scaffold (H&E staining; ×200 magnification). (**B**) Cells in the multilayer structure showing Toluidine/Fast Green–positive staining (marked with arrows). Purple staining indicates the presence of acid mucopolysaccharides (glycosaminoglycans) (×400 magnification). (**C**) Few spindle-shaped cells visible inside and on the surface of the Degrapol scaffolds (H&E staining; ×100 magnification). (**D**) Negative Toluidine/Fast Green staining (×400 magnification). These results show improved three-dimensional chondrocyte growth and extracellular matrix formation in F12 medium without Oxygent.

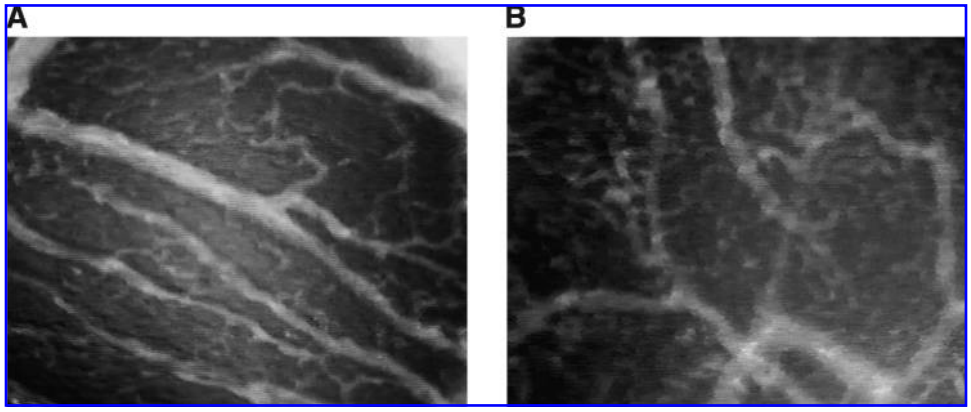

FIG. 6. OPS imaging analysis showed no significant difference regarding the functional capillary density around ADM scaffolds (**A**) versus Oxygent–ADM scaffolds (**B**). OPS imaging, orthogonal polarization spectral imaging; ADM, acellular dermis matrix.

In contrast to the benefits seen on the tracheal epithelium, the Oxygent- containing medium caused an initial decrease in viability and function of immersed chondrocyte–DegraPol construct. This finding, shown on histology and in the reduced GAG production, may have been caused by a direct interaction of the PFC surfactant with cell membrane proteins, thereby interfering with proper chondrocyte differentiation.[29,30] Cartilage tissue proved critical to provide enough mechanism strength preventing tracheal malacia. Interestingly, several other published studies using PFC emulsions have described positive effects on cell growth and differentiation in various cell culture systems.[31–34] These divergent results call for additional detailed investigations to establish the optimal biocompatible concentration of artificial oxygen carriers to be used as perfusates in tissue engineering with emphasis on long-term effect.

One alternative might be to prevent chondrocyte–DegraPol construct from direct Oxygent contact, which means that in the later *in vivo* bioreactor design application the perfusate with artificial oxygen carrier will be limited in epithelial and submucous layers. It should be feasible because cartilage tissue is physically avascular and get nutrients from diffusion of tissue fluid. In normal tracheal construction, cartilage rings are isolated from submucous tissue by fibrous membrane. The other alternative lies in the combination of the Oxygent to the TET epithelial scaffold to decrease the perfusion concentration. To test whether the Oxygent combination may negatively interfere with the tissue reactions of TET, ADM scaffolds preexposed to medium with/without Oxygent were transplanted onto the vascularized CAMs of the chick embryo and cultured for up to 10 days. OPS imaging showed no impairment of angiogenesis in the CAM–TET transplant interface in both experimental conditions, indicating that the use of Oxygent was compatible with the biologically important graft neovascularization. The use of noninvasive OPS imaging for monitoring the microcirculation and functional capillary density in the CAM model eliminated the need for injecting fluorescent dyes, which is technically demanding and may cause extravasations. OPS imaging has already been validated against the dynamic intravital fluor-

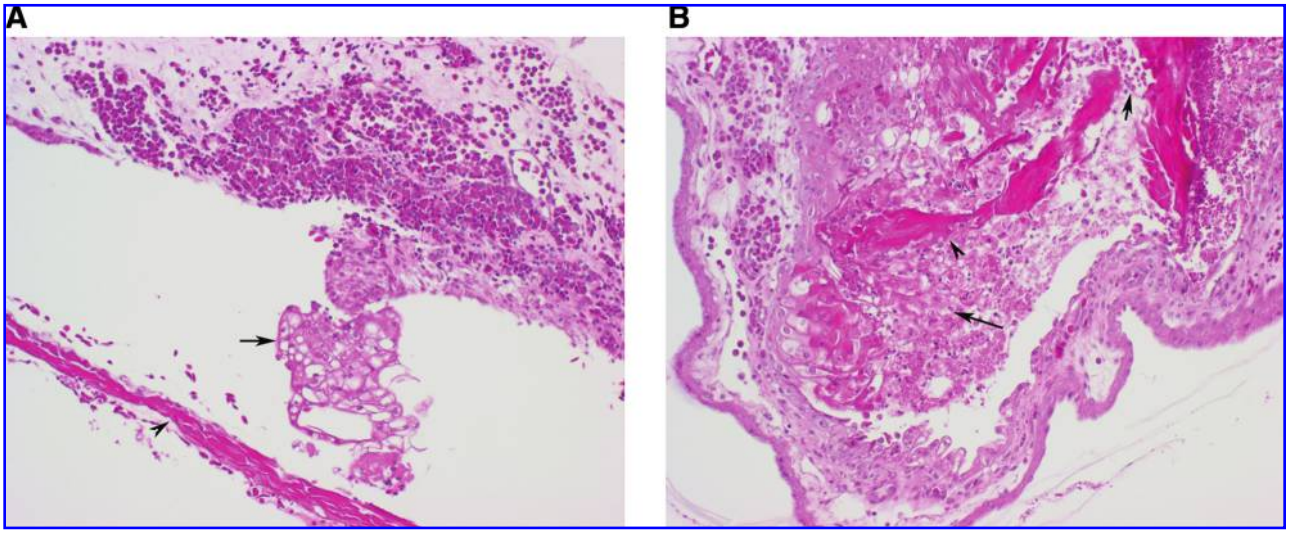

FIG. 7. Histological changes of a foreign body reaction to ADM–CAM transplants. (**A**) Ballooning degeneration (marked with arrow) of chorioallantoic epithelium in contact with ADM (marked with arrowhead) (×200 magnification). (**B**) Part of the scaffold (marked with arrowhead) was engulfed into the mesoderm and surrounded with heterophilic leukocytes (marked with short arrow) and macrophages (marked with long arrow, indicating foreign body reaction) (×200 magnifications). CAM, chorioallantoic membrane. Color images available online at www.liebertonline.com/ten.

omicroscopy in skin-fold preparation of hamster and liver microcirculation in rats.[19,35] Histological results also proved no compromise regarding biocompatibility with Oxygent combination.

In conclusion, the artificial oxygen carrier Oxygent significantly increased the epithelial PtO_2 in TET epithelium, improved tracheal epithelial metabolism, did not impair CAM angiogenesis in ADM, and was biocompatible. However, in chondrocyte–DegraPol construct, Oxygent deposits interfered with chondrocyte metabolism, which needs further investigations. For future *in vivo* bioreactor applications, Oxygent may be used systemically as a supplement to the perfusate and/or topically integrated into appropriate biomatrices.

Acknowledgments

This study was supported by Swiss National Foundation (NFP 116807). We faithfully appreciate Dr. Peter Neuenschwander and Dr. Yingen Pan for the supply of DegraPol and ADM scaffolds, respectively. The human tracheal epithelial cell line 16HBE14o was generously provided by Dr. Jordi Ehrenfeld, Faculte des Sciences de Nice, France.

Disclosure Statement

No competing financial interests exist.

References

1. Grillo, H.C. The history of tracheal surgery. Chest Surg Clin N Am **13,** 175, 2003.
2. Malda, J., Klein, T.J., and Upton, Z. The roles of hypoxia in the *in vitro* engineering of tissues. Tissue Eng **13,** 2153, 2007.
3. Landman, K.A., and Cai, A.Q. Cell proliferation and oxygen diffusion in a vascularising scaffold. Bull Math Biol **69,** 2405, 2007.
4. Potier, E., Ferreira, E., Meunier, A., Sedel, L., Logeart-Avramoglou, D., and Petite, H. Prolonged hypoxia concomitant with serum deprivation induces massive human mesenchymal stem cell death. Tissue Eng **13,** 1325, 2007.
5. Brown, D.A., Maclellan, W.R., Wu, B.M., and Beygui, R.E. Analysis of pH gradients resulting from mass transport limitations in engineered heart tissue. Ann Biomed Eng **35,** 1885, 2007.
6. Brown, D.A., Maclellan, W.R., Laks, H., Dunn, J.C., Wu, B.M., and Beygui, R.E. Analysis of oxygen transport in a diffusion-limited model of engineered heart tissue. Biotechnol Bioeng **97,** 962, 2007.
7. Smith, M.K., and Mooney, D.J. Hypoxia leads to necrotic hepatocyte death. J Biomed Mater Res A **80,** 520, 2007.
8. Radisic, M., Deen, W., Langer, R., and Vunjak-Novakovic, G. Mathematical model of oxygen distribution in engineered cardiac tissue with parallel channel array perfused with culture medium containing oxygen carriers. Am J Physiol Heart Circ Physiol **288,** 1278, 2005.
9. Tan, Q., Steiner, R., Yang, L., Welti, M., Neuenschwander, P., Hillinger, S., and Weder, W. Accelerated angiogenesis by continuous medium flow with vascular endothelial growth factor inside tissue-engineered trachea. Eur J Cardiothorac Surg **31,** 806, 2007.
10. Tan, Q., Steiner, R., Heorstrup, S.P., and Weder, W. Tissue-engineered trachea: history, problems and the future. Eur J Cardiothorac Surg **30,** 782, 2006.
11. Keipert, P.E. Perflubron emulsion (Oxygent™): a temporary intravenous oxygen carrier. Anasthesiol Intensivmed Notfallmed Schmerzther **36,** 104, 2001.
12. Kemming, G.I., Meisner, F.G., Wojtczyk, C.J., Packert, K.B., Minor, T., Thiel, M., Tillmanns, J., Meier, J., Bottino, D., Keipert, P.E., Faithfull, S., and Habler, O.P. Oxygent™ as a top load to colloid and hyperoxia is more effective in resuscitation from hemorrhagic shock than colloid and hyperoxia alone. Shock **24,** 245, 2005.
13. Morris, K., Cox, P., Frndova, H., Holowka, S., and Babyn, P. Effect of a sustained inflation on regional distribution of gas and perfluorocarbon during partial liquid ventilation. Pediatr Pulmonol **42,** 204, 2007.
14. Lowe, K.C. Engineering blood: synthetic substitutes from fluorinated compounds. Tissue Eng **9,** 389, 2003.
15. Boubriak, O.A., Urban, J.P., and Cui, Z. Monitoring of metabolite gradients in tissue-engineered constructs. J R Soc Interface **3,** 637, 2006.
16. Boubrak, O.A., Urban, J.P., and Cui, Z. Monitoring of lactate and glucose levels in engineered cartilage construct by microdialysis. J Memb Sci **273,** 77, 2006.
17. Zwadlo-Klarwasser, G., Goerlitz, K., Hafemann, B., Klee, D., and Klosterhalfen, B. The chorioallantoic membrane of the chick embryo as a simple model for the study of the angiogenic and inflammatory response to biomaterials. J Mater Sci Mater Med **12,** 195, 2001.
18. Klueh, U., Dorsky, D.I., Moussy, F., and Kreutzer, D.L. Ex ova chick chorioallantoic membrane as a novel model for evaluation of tissue responses to biomaterials and implants. J Biomed Mater Res A **67,** 838, 2003.
19. Langer, S., Harris, A.G., Biberthaler, P., von Dobschuetz, E., and Messmer, K. Orthogonal polarization spectral imaging as a tool for the assessment of hepatic microcirculation: a validation study. Transplantation **71,** 1249, 2000.
20. Landers, R., Huebner, U., Schmelzeisen, R., and Muelhaupt, R. Rapid prototyping of scaffolds derived from thermoreversible hydrogels and tailored for applications in tissue engineering. Biomaterials **23,** 4437, 2002.
21. Yang, L., Korom, S., Welti, M., Hoerstrup, S.P., Zund, G., Jung, F.J., Neuenschwander, P., and Weder, W. Tissue engineered cartilage generated from human trachea using Degrapol scaffold. Eur J Cardiothorac Surg **24,** 201, 2003.
22. Feng, X., Tan, J., Pan, Y., Wu, Q., Ruan, S., Shen, R., Chen, X., and Du, Y. Control of hypertrophic scar from inception by using xenogenic (porcine) acellular dermal matrix (ADM) to cover deep second degree burn. Burns **32,** 293, 2006.
23. Contaldo, C., Harder, Y., Plock, J., Banic, A., Jakob, S.M., and Erni, D. The influence of local and systemic preconditioning on oxygenation, metabolism and survival in critically ischaemic skin flaps in pigs. J Plast Reconstr Aesthet Surg **60,** 1182, 2007.
24. Moroni, L., Curti, M., Welti, M., Korom, S., Weder, W., de Wijn, J.R., and van Blitterswijk, C.A. Anatomical 3D fiber-deposited scaffolds for tissue engineering: designing a neotrachea. Tissue Eng **13,** 2483, 2007.
25. Steiner, R. Angiostatic activity of anticancer agents in the chick embryo chorioallantoic assay. In: Steiner, R., Weisz, B.P., and Langer, R., eds. Angiogenesis: Key Principles–Science–Technology–Medicine. Basel, Switzerland: Birkhauser, 1992, pp. 449–454.
26. Contaldo, C., Meier, C., Elsherbiny, A., Harder, Y., Trentz, O., Menger, M.D., and Wanner, G.A. Human recombinant erythropoietin protects the striated muscle microcirculation

of the dorsal skinfold from postischemic injury in mice. Am J Physiol Heart Circ Physiol **293,** 274, 2007.
27. Schultz, P., Vautier, D., Charpiot, A., Lavalle, P., and Debry, C. Development of tracheal prostheses made of porous titanium a study on sheep. Eur Arch Otorhinolaryngol **264,** 433, 2007.
28. Riess, J.G. Oxygen carriers ("blood substitutes")—raison d'etre, chemistry, and some physiology. Chem Rev **101,** 2797, 2001.
29. Lowe, K.C., Davey, M.R., and Power, J.B. Perfluorochemicals: their applications and benefits to cell culture. Trends Biotechnol **16,** 272, 1998.
30. Centis, V., Doillon, C.J., and Vermette, P. Perfluorocarbon emulsions cytotoxic effects on human fibroblasts and effect of aging on particle size distribution. Artif Organs **31,** 649, 2007.
31. Lowe, K.C. Perfluorochemical respiratory gas carriers: benefits to cell culture systems. J Fluor Chem **118,** 19, 2002.
32. Davey, M.R., Anthony, P., Power, J.B., and Lowe, K.C. Applications and benefits of a non-ionic surfactant and artificial oxygen carriers for enhancing post-thaw recovery of plant cells from cryopreservation. Adv Exp Med Biol **540,** 139, 2003.
33. Tsujimura, T., Kuroda, Y., Avila, J.G., Kin, T., Oberholzer, J., Shapiro, A.M., and Lakey, J.R. Influence of pancreas preservation on human islet isolation outcomes: impact of the two-layer method. Transplantation **78,** 96, 2004.
34. Nahmias, Y., Kramvis, Y., Barbe, L., Casali, M., Berthiaume, F., and Yarmush, M.L. A novel formulation of oxygen-carrying matrix enhances liver-specific function of cultured hepatocytes. FASEB J **20,** 2531, 2006.
35. Groner, W., Winkelman, J.W., Harris, A.G., Ince, C., Bouma, G.J., Messmer, K., and Nadeau, R.G. Orthogonal polarization spectral imaging: a new method for study of the microcirculation. Nat Med **5,** 1209, 1999.

Address reprint requests to:
Walter Weder, M.D.
Department of Thoracic Surgery
University Hospital Zurich
Raemistrasse 100
CH-8091 Zurich
Switzerland

E-mail: walter.weder@usz.ch

Received: August 11, 2008
Accepted: January 22, 2009
Online Publication Date: March 3, 2009